

Strength of thermoplastic elastomers from rubber-polyolefin blends

NAMITA ROY CHOUDHURY, ANIL K. BHOWMICK*

Rubber Technology Centre, Indian Institute of Technology, Kharagpur 721 302, India

The strength of different thermoplastic elastomers of varying compositions and interactions has been examined over a wide range of rates and temperatures and for a wide variety of test configurations. Fracture energy was calculated from various test specimens and found to be similar, and independent of the test configuration. Fracture energy values lie between 0.8 and 120 kJ m⁻². The behaviour could be compared with that of rubbers. However, for a trouser-tear test piece, the fracture energy increases with increasing thickness of the torn path in the very small thickness region, as for the fracture of polyethylene. The fracture surface morphology of various composites indicates different mechanisms of crack propagation. The tensile rupture data over a wide range of rates and temperatures could be represented by a single parabolic curve – the “failure envelope”. The maximum elongation at break and tensile strength of the composites are related to the modulus.

1. Introduction

Thermoplastic elastomers are of relatively recent origin. These are replacing many conventional rubber parts because the processes involved in their production are less energy intensive. A few rubber-polyolefin blends have been commercialized with the same purpose in mind, and many more composites are still in the research stage. Surprisingly, little information is available on the strength properties of thermoplastic elastomeric rubber-plastic blends. It would be interesting to know whether tear and tensile strengths are strongly dependent upon the rate of tearing and the temperature of the test, as would be expected for viscoelastic materials such as rubber, whether the measured fracture energy is characteristic of the material and independent of the test method as observed for rubbers, and what role the interaction between the components plays in determining the strength of these materials. The results of our investigation on the above questions are presented here, with reference to natural rubber-polyethylene, natural rubber-polypropylene, ethylene propylene diene-polyethylene, ethylene propylene diene-polypropylene and nitrile rubber-polypropylene blends. The materials were chosen in such a way that there was a wide variation in composition and interaction.

The effect of interaction promoter on the technical properties and morphology of these blends has been reported earlier [1]. Preparation, properties and application of various thermoplastic elastomers have been covered recently [2]. Rivlin and Thomas [3] and Thomas [4] have shown that for a wide variety of rubber test specimens, values of fracture energy are independent of the test piece and dependent upon the

rate of tearing and test temperature. However, Ahagon *et al.* [5] later observed, that torn surfaces of rubber undergoing a shear displacement yield substantially higher values of fracture energy than those in which torn surfaces move apart with the progress of the tear. Anderton and Treloar [6] examined the effect of orientation on the tear strength of low and high-density polyethylene. Sims [7] found a value of 120 kJ m⁻² at 20°C for his studies on unoriented films of polyethylene. Vincent [8] measured the fracture energy of unoriented polyethylene terephthalate (resembling polyethylene in ductility). Bhowmick and Gent [9] and Bhowmick [10] measured the tensile and tear strength of rubbers over a range of cross-linking density, test rates and temperatures. Smith [11, 12] has demonstrated failure envelopes from stress and strain data at various rates and temperatures of different rubbers and thermoplastic block copolymers.

It is well known from the above studies that the strain energy, ϵ , is assumed to decrease with cut length, c [13] on the basis of the volume of material released from strain around the crack

$$\epsilon = \epsilon^0 - \epsilon' \quad (1)$$

where ϵ^0 is the strain energy for a test piece containing no cut, ϵ' is the strain energy decrease due to a cut.

For a tensile dumb-bell, as shown in Fig. 1a,

$$\epsilon' = kc^2tW \quad (2)$$

where W is the strain energy density, t the thickness of the rubber, c the crack length, k a numerical quantity, given by π for infinitesimal strains and by $\pi(1 + e)^{-1/2}$, approximately, for materials subjected to a finite tensile strain, e .

* Author to whom all correspondence should be addressed.

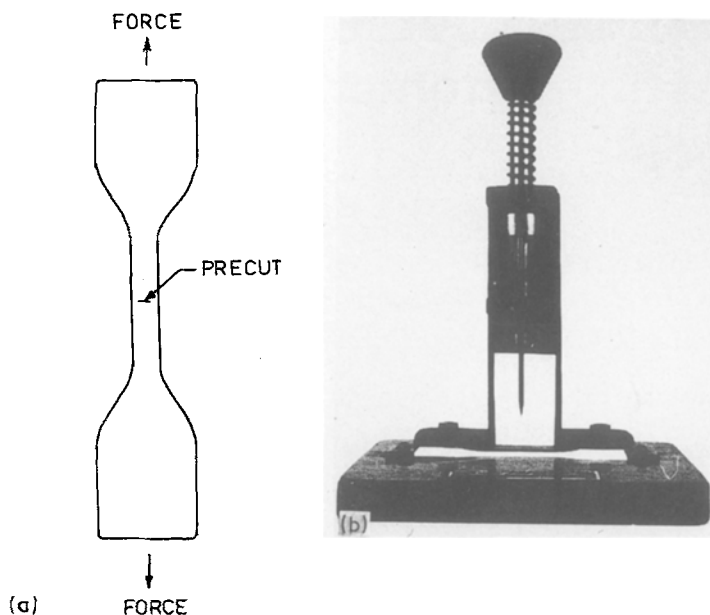


Figure 1 (a) Sketch of a tensile test specimen. (b) The shape of the jig.

The critical energy release rate, G_c , is defined as

$$G_c = - \left(\frac{\delta \epsilon}{\delta A} \right)_{\text{fracture}} \quad (3)$$

where A is the area of the torn surface.

Combining Equations 1, 2 and 3

$$G_{c, \text{tensile}} = 2kcW \quad (4)$$

For a pure shear test piece (Fig. 2)

$$\epsilon' = cthW \quad (5)$$

where h is the unstrained height of the test piece and c is sufficiently large.

Combining Equations 1, 3 and 5

$$G_{c, \text{shear}} = hW \quad (6)$$

Similarly, for a tear test piece shown in Fig. 3a

$$G_{c, \text{tear}} = \frac{2F}{t'} \quad (7)$$

where t' is the width of the torn path and F is the tear force. It has been observed that for general-purpose rubber

$$G_{c, \text{tensile}} = G_{c, \text{shear}} = G_{c, \text{tear}} \quad (8)$$

The above relation will be tested here for thermoplastic elastomers comprising rubber and plastic.

2. Experimental details

The formulations of the various mixes are given in Table I. Mixing and moulding were carried out as reported earlier [1].

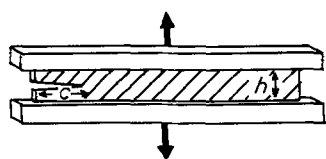


Figure 2 Sketch of a shear test specimen.

2.1. Materials

Natural rubber (NR) – ISNR 5, was supplied by Rubber Board, Kottayam, India: molecular weight, $M_w = 780\,000$; intrinsic viscosity (benzene, 30°C) (η) = 4.45 dl g^{-1} ; Wallace plasticity, $q_0 = 59.0$.

Polyethylene (PE) – Indothene 16 MA 400, was supplied by IPCL, Baroda: density = 0.916 g cm^{-3} ; melt flow index, MFI = 40 g/10 min .

Polypropylene (PP) – Koylene M0030, was supplied by IPCL, Baroda: molecular weight, $M_w = 530\,000$; density = 0.910 g cm^{-3} ; melt flow index (230°C and 2.16 kg), MFI = 10 .

Chlorinated polyethylene (CPE) – 36% chlorine, was supplied by Dow Chemicals, USA: specific gravity = 1.16 ; Mooney viscosity $ML_{(1+4)} 121^\circ\text{C} = 80$.

Ethylene propylene diene Rubber (EPDM) – Keltan 520, was supplied by DSM, Holland through SBM Chemicals, India: specific gravity = 0.86 ; Mooney viscosity $ML_{(1+4)} 125^\circ\text{C} = 46$.

Epoxidized natural rubber (ENR) – ENR 25, was supplied by MRPRA, UK: density = 0.97 g cm^{-3} ;

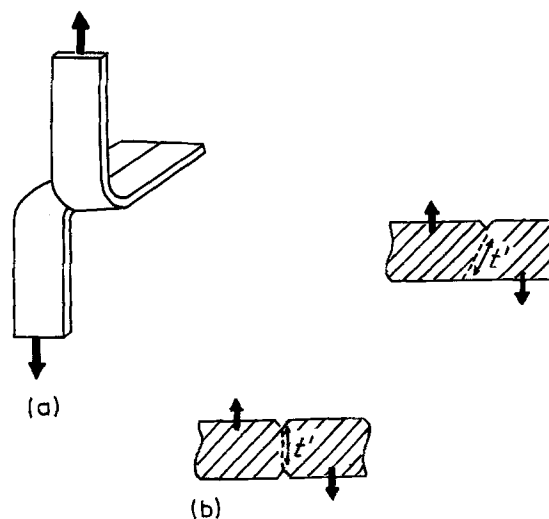


Figure 3 Sketches of (a) trouser-tear test specimen, (b) trouser tear specimen scored on both sides.

TABLE I Formulation of the mixes

Blend components	A	B	C	D	E	F	G	H
NR	70	70	70	—	—	—	70	70
CPE	—	—	20	—	—	—	—	—
ENR	—	—	—	—	—	—	20	—
EPDM	—	—	—	70	70	—	—	—
NBR	—	—	—	—	—	70	—	—
PE	30	30	30	30	—	—	27	27
PE _m	—	—	—	—	—	—	3	3
PP	—	—	—	—	30	30	—	—
DCP	0.5	—	0.5	—	—	—	—	0.5
ZnO	—	5	—	5	5	5	—	—
Stearic acid	—	1	—	1	1	1	—	—
S	—	2.5	—	2	2	2	—	—
CBS	—	0.8	—	—	—	—	—	—
TMTD	—	—	—	1	1	—	—	—
MBTS	—	—	—	0.5	0.5	0.55	—	—

epoxidation level 25 mol %; Mooney viscosity $ML_{(1+4)}$ $100^\circ C = 110$.

Nitrile rubber (NBR) was supplied by Dunlop India Ltd, Sahaganj: acrylonitrile content 34%; Mooney viscosity $ML_{(1+4)}$ at $100^\circ C = 50$; specific gravity = 0.98.

DCP — dicumyl peroxide, was supplied by Hercules Incorporated, Wilmington, USA.

ZnO — zinc oxide; specific gravity = 5.55.

Stearic acid; specific gravity = 0.85.

S — sulphur; density = 1.9 g cm^{-3} .

CBS — cyclohexyl benzthiazyl sulphenamide, was supplied by IEL, Rishra, Hooghly: specific gravity at $25^\circ C = 1.30$; melting point $101^\circ C$.

MBTS — 2-benzothiazyl disulphide, was supplied by IEL, Rishra, Hooghly: specific gravity at $25^\circ C = 1.54$; melting point $167^\circ C$.

TMTD — tetramethyl thiuram disulphide, was supplied by IEL, Rishra, Hooghly: specific gravity at $25^\circ C = 1.42$; melting point $140^\circ C$.

2.2. Measurement of fracture energy

Various test specimens as shown in Figs 1 to 3 have been used to determine the fracture energy, which is calculated using Equations 4, 6 and 7. Tensile strength was measured using a dumb-bell specimen as per ASTM method D412-80. The strain energy density, was calculated from the area under the stress-strain curve.

Strength values were measured in a Zwick Universal testing machine (model 1445) over a wide range of temperatures and rates. The width of the torn path (for test specimens in Figs 3a and b) was measured using a travelling microscope. Various lengths of cut were introduced into the tensile samples using a jig, as shown in Fig. 1b. Three samples were tested in each case and the experimental error was within $\pm 15\%$.

2.3. Measurement of elastic modulus

The small strain modulus of various thermoplastic elastomers has been measured in tension and obtained from the initial slope of the stress-strain curve. The error in this experiment is $\pm 5\%$ on three samples.

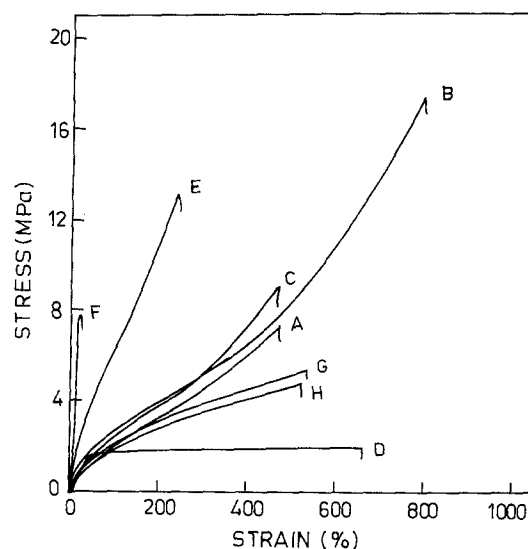


Figure 4 Stress-strain curves of the blends.

2.4. Fracture surface morphology

The fractured surfaces of all the samples were sputter-coated with gold before examination under a scanning electron microscope (Phillips SEM 500 model).

3. Results and discussion

3.1. Characterization of composites

The stress-strain properties of various composites are shown in Fig. 4. The compositions chosen in the present study are based on natural rubber-polyethylene, ethylene propylene diene rubber-polyethylene and EPDM-polypropylene and nitrile rubber-polypropylene systems. As observed in Fig. 4, the small strain moduli of various materials are in the range of 21 to 60 kPa. The tensile strength of mix B is highest while that of mix D is the lowest. The elongation at break is lowest for mix F. The interaction between natural rubber and polyethylene has also been varied by choosing the interaction promoter — both physical and chemical in nature. For example, EPDM acts as a physical interfacial agent, whereas ENR and PE_m reacts chemically at the interface. We have already reported the technical properties of various composites with reference to interaction between components [1, 14].

3.2. Fracture energy of thermoplastic elastomers for a wide variety of test configurations

Fracture energy of thermoplastic elastomers under various test configurations is reported in Table II. Tensile test specimens with two lengths of cut (Fig. 1), shear specimen (Fig. 2) and trouser-tear specimen (Fig. 3) were used. As shown in Table II, with the exception of composition C, values of fracture energy determined in different ways are similar for a wide range of compositions differing in modulus and interaction. Composition C, comprising NR/CPE/PE/DCP, shows a considerably lower value ($\sim 50\%$) measured in the trouser-tear mode (Fig. 3), though the tensile specimen, having different cut lengths, and the shear specimen show almost identical values. When the shearing is constrained at 0° for the trouser-test

TABLE II Modulus, tensile strength and tearing energy values of different blends at room temperature

Blends	Modulus, E (kPa)	Tensile strength (MPa)	$G_{c1, tensile}^*$ (kJ m^{-2})	$G_{c2, tensile}^\dagger$ (kJ m^{-2})	$G_{c, shear}^\ddagger$ (kJ m^{-2})	$G_{c, tear}^\S$ (kJ m^{-2})
A	30	6.4	18.0	17.5	19.0	17.0
B	54	15.5	120.0	120.0	—	120.0 (130)
C	42	8.4	28.0	29.7	28.2	12.0 (30.0)
D	24	1.5	14.0	13.0	12.5	15.0
E	60	12.3	28.0	29.5	27.0	28.0
F	21	7.9	0.5	0.8	—	0.6
G	35	5.2	15.0	15.3	18.0	19.8 (16.0)
H	30	5.3	15.0	15.0	13.0	15.0

*Tearing energy with cut length of 1.36 mm.

† Tearing energy with cut length of 0.46 mm.

‡ Tearing energy for shear specimens.

§ Tearing energy for trouser specimen.

|| Values in parentheses indicate tearing energy measured as per Fig. 3b.

specimen, as was done by Ahagon *et al.* [5], the values are considerably improved, probably due to the fact that the tear path follows a zig-zag cross-section. This has been attributed by Chiu *et al.* [15] to the frictional work expended in sliding the rough torn surfaces past each other. However, for other materials such as G and B, all the specimens (Figs 1 to 3) yield similar values of tearing energy. It is observed that the mechanism of crack propagation (which is discussed in a later section) is different for different materials. It is observed, moreover, for all the thermoplastic materials studied, that the fracture energy is a more fundamental measure of strength and is characteristic of the material. Also, the behaviour is very similar to rubber. It is, however, not a single-value property and does depend on the rate of tearing and test temperature, as observed for rubbery material. The effects of test rates and temperatures of some representative materials is shown in Figs 5 and 6. The variation in rate or temperature is similar to that discussed earlier [11, 12]. The tearing energy is lower at higher temperatures and

lower rates of tear propagation. These are related to the viscoelasticity of the composites.

3.3. Fracture energy of various thermoplastic elastomers

The fracture energies of various thermoplastic elastomers are also reported in Table II. It has been observed that composition B has the highest tearing energy, while composition F has the lowest. Other compositions have intermediate values. Compositions A, D, G and H have comparable values; blends C and E show similar behaviour. The relative trend in tearing energy of the various compositions studied is not in line with the trend in tensile strength reported in the same table: the tensile strength of B is close to that of E, while the tearing energy of B is more than four times higher. The tensile strengths of D and G are widely different, yet the tearing energies are comparable. The difference in strength values in these two measurements may be ascribed to different rates of tear propagation in the two processes. In one case the

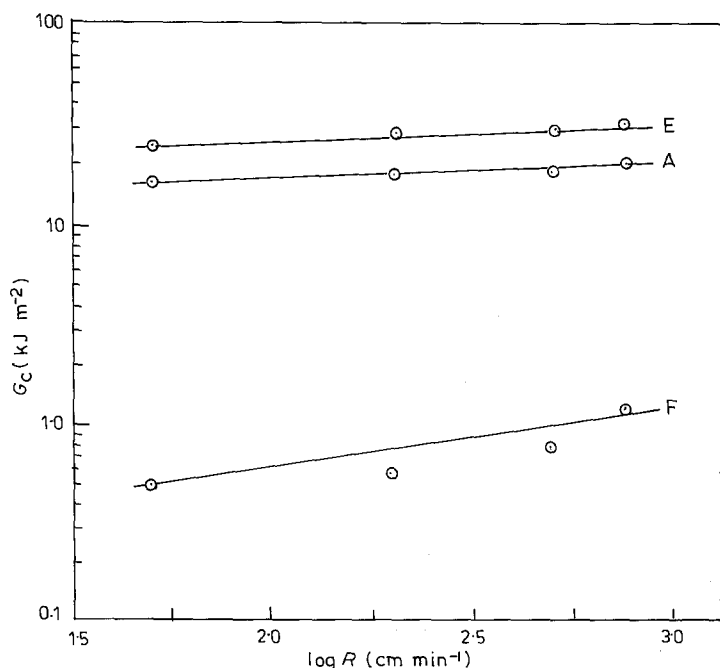


Figure 5 Logarithmic plot of tearing energy, G_c against rate, R .

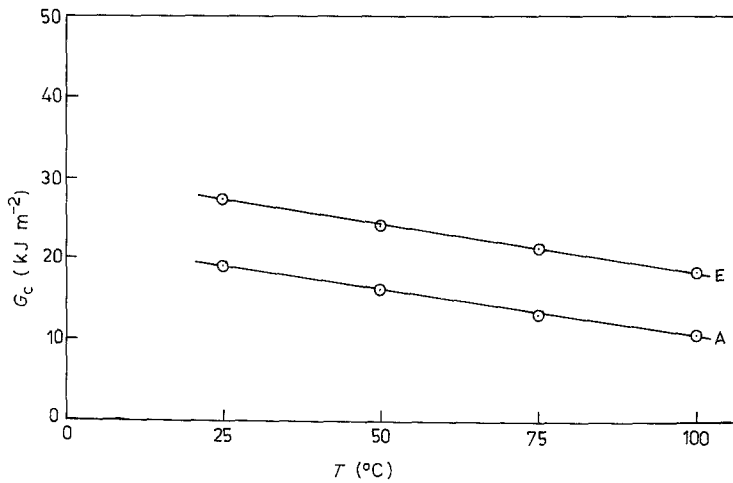


Figure 6 Plot of tearing energy, G_c against temperature, T .

total energy is concentrated at the tip of the crack, while in the other the deformation of the whole specimen becomes important. Even for dumb-bell samples with a precut, the supplied energy seems to be concentrated at the crack tip.

The fracture energy of these materials is comparable to that of carbon black-filled or strain-crystallizing elastomer, for a tear rate of 1 mm sec^{-1} at room temperature. This remarkably high value is attributed to plastic flow of a hard phase under high stress and dissipation of strain energy as a result.

3.4. Effect of width of the tear path on fracture energy for test piece type 3

It has been reported by Chiu *et al.* [15] that the fracture energy of moulded sheets of polyethylene depends on the thickness of the sheet, because of the dependence of the volume of the plastic zone at the crack tip. Test pieces (Type 3) were scored in the middle to different widths of tear path from thickness 0.05 to 0.24 cm. As shown in Fig. 7, the fracture energy is plotted against cut thickness for composition C. At very small thickness ($< 0.10 \text{ cm}$) the tear energy does depend on the thickness, whereas at higher thickness ($> 0.10 \text{ cm}$), the

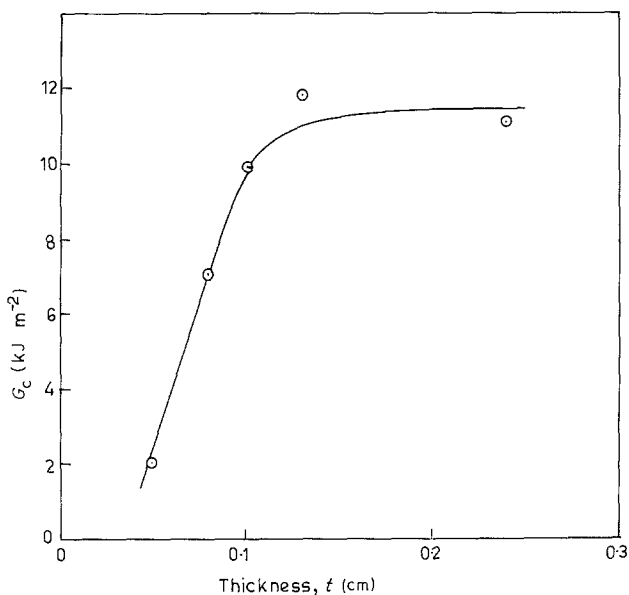


Figure 7 Variation of tearing energy, G_c against thickness, t , for blend C.

fracture energy is independent of thickness. All the fracture energy measurements have been done at thicknesses greater than 0.10 cm in our present experiment. The variation may be attributed to (i) a dependence of the volume of plastic zone at the crack tip on torn thickness as suggested by Chiu *et al.* [15] for polyethylene; (ii) limited deformation of the plastic phase under low local stress when the width is very small, below 0.1 cm.

However, Chiu *et al.* [15] observed a strong dependence of tearing energy on thickness (t^2) even at higher thickness. In the present experiment, a plateau is observed after a certain thickness. The effect of thickness on strength properties is a combined effect — at low thickness the behaviour is similar to that of plastics whereas at high thickness this is like that of rubbers.

3.5. Fracture surface morphology

In order to understand the mechanism of fracture of a variety of thermoplastic rubbers, we have studied the fracture surface morphology, which represents pictorially the crack propagation in the matrix. SEM observations are shown in Figs 8a to d at low magnifications ($\times 50$ and $\times 100$) for comparison. While the highest strength of matrix B (Fig. 8a) is associated with ductility and dimples, the low strength of matrix F (Fig. 8b) results from the fibrous and brittle characteristics with long fissures on the fracture surface. The fracture surface of other compositions has also been examined. It is difficult to predict the order of tearing energy of the matrix on the basis of surface morphology. However, it could be concluded that the mechanisms of crack propagation for various materials are different. For example, compositions D and E (Figs 8c and d) show brittle fracture, as compared to B (Fig. 8a). The crack lines and flow lines are clearly observed on the surface. In the EPDM/PE system (Fig. 8c), the PE matrix is deformed and curled. The EPDM/PP matrix (Fig. 8d) shows platelet features, characteristic of brittle materials. Recently, Saha Deuri and Bhowmick [16] correlated the spacing between observed tear lines and crack lines with the strength of EPDM, natural rubber and butadiene rubber vulcanizates. Such a correlation could not be done here with the limited fractographs.

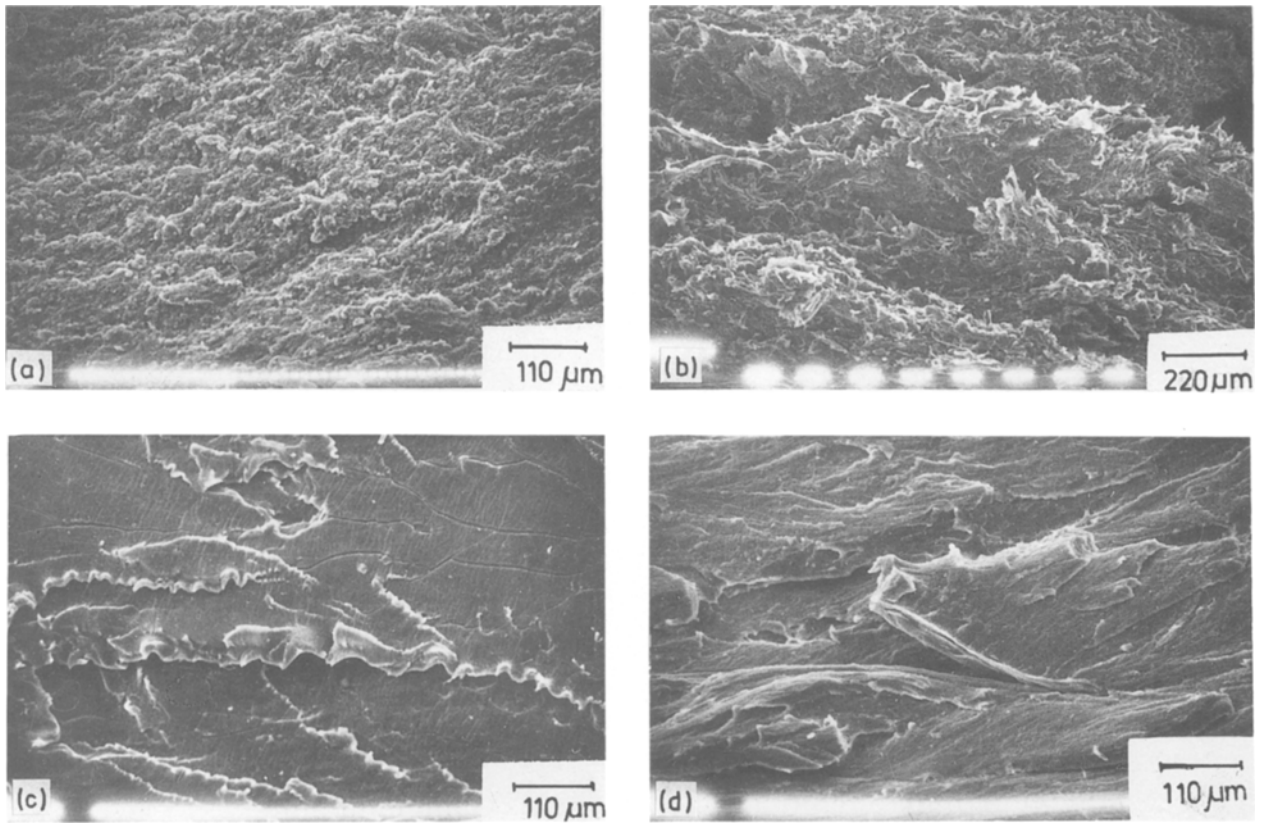


Figure 8 (a) Tensile fractographs of blends (a) B, (b) F, (c) D and (d) E. (500 mm min^{-1} rate of test at room temperature.)

3.6. Tensile strength of thermoplastic rubber over a range of rates and temperatures

The tensile strength of thermoplastic rubbers over a range of rates and temperatures has been measured and the data are plotted against the elongation at break in Fig. 9. A small correction factor ($298/T$, where T is the test temperature) has been multiplied by the measured σ_b values to allow for changes in elastic modulus with temperature. It has been observed that the data yield a single parabolic curve. This has been termed the "failure envelope" by Smith [17]. It is

interesting to note that the variation in strength properties with rate or temperature is similar to rubber. Curve B in Fig. 9 indicates the maximum breaking elongation, $e_{b,max}$. There are two extremes — one corresponding to an increase in strength with increase in breaking extension, obtained at high temperatures, and low strain rates, and the other showing high breaking stress and low extensibility.

Because the rate of crack growth prior to catastrophic propagation is controlled by the viscous characteristics of the material, both the tensile strength

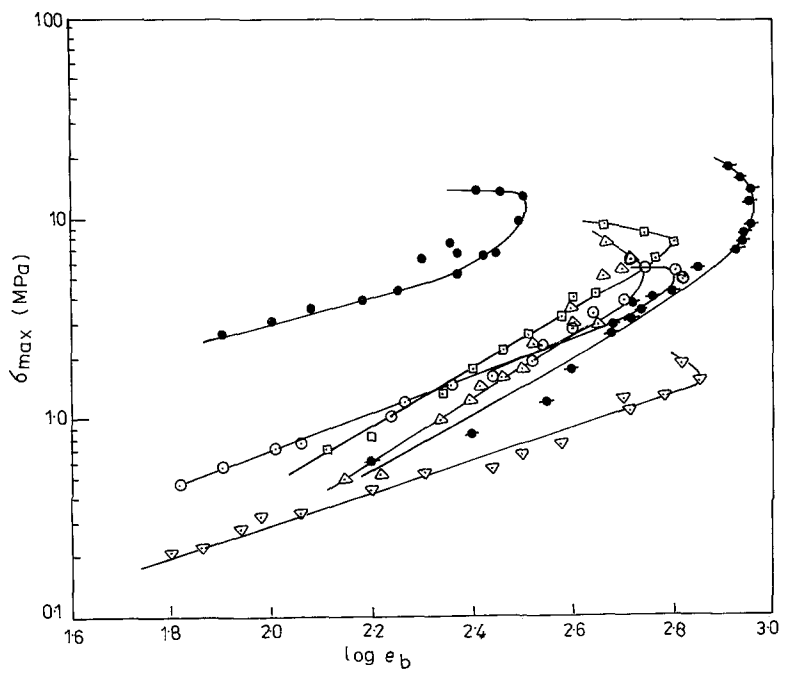


Figure 9 "Failure envelope" of various mixes: (Δ) A; (\bullet) B; (\square) C; (∇) D, (\bullet) E, (\circ) G.

and ultimate extension depend on temperatures and extension rates as for rubbers. The breaking elongation at first increases with increasing stress and then falls at higher rates as the chain segments are unable to respond sufficiently. Smith [17] has reviewed strength properties of styrene-butadiene rubber, fluorohydrocarbon, natural rubber, butyl rubber and polyurethane block copolymer and discussed the role of viscoelasticity on failure envelopes.

It may be observed from Fig. 9 that the materials differ in maximum breaking extensibility. Composition B shows the highest value, and material E the lowest. In order to understand the behaviour of the materials with a basic property, $e_{b,max}$ and (σ_b) at $e_{b,max}$, i.e. σ'_{max} have been plotted in Figs 10 and 11 against the modulus, E . While σ'_{max} increases with increasing E , $(1 + e_{b,max})^2$ decreases with E (the fit is not very good). Hence

$$\sigma'_{max} \propto E \quad (9)$$

$$(1 + e_{b,max})^2 \propto 1/E \quad (10)$$

It has been demonstrated earlier for rubbers that

$$(1 + e_{b,max}) \propto M_c^{1/2} \quad (11)$$

where $(1/2M_c)$ is the cross-link density of the material.

It can be understood now from the relationship between maximum breaking elongation and E that the plastics act as physical cross-links and the strength properties are indirectly related to the modulus of the plastic phase and morphology of the blends. The morphology of various materials, as reported earlier, is widely different for the various blend compositions. Even if the morphology is different, the hard plastic phase deforms before the actual rupture. The tensile strengths of A and B, which vary only in dynamic curing systems, are different, although the adhesion between natural rubber and polyethylene is the same.

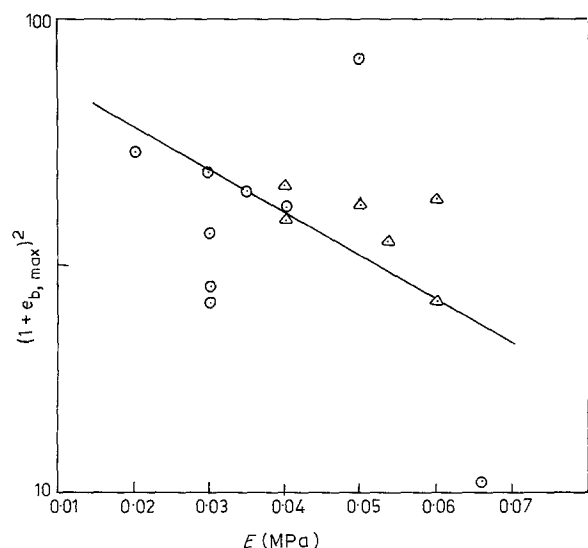


Figure 10 Plot of $(1 + e_{b,max})^2$ against modulus E (C) values for the blends A to H; (Δ) values for the modified systems (NR/PE_m/PE, NR/CPE/PE_m/PE, NR/S-EPDM/PE, NR/S-EPDM/PE_m/PE, NR/ENR/PE, NR/ENR/PE_m/PE).

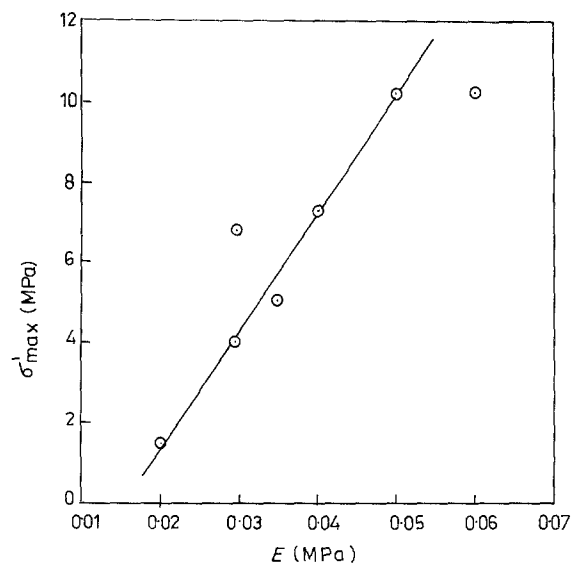


Figure 11 Plot of σ'_{max} against modulus E .

This is also true for tearing energy values. It indicates that the dissipation of strain energy at the crack tip is as important as adhesion between components. Detailed studies on the relation between adhesion, hysteresis and tearing are in progress in this laboratory.

Acknowledgement

The authors thank the Department of Science and Technology, New Delhi for funding the project.

References

1. N. ROY CHOUDHURY and A. K. BHOWMICK, *J. Mater. Sci.* **23** (1988) 2187.
2. A. Y. CORAN, in "Handbook of Elastomers - New Development and Technology", edited by A. K. Bhowmick and H. L. Stephens (Marcel Dekker, New York, 1988) p. 249.
3. R. S. RIVLIN and A. G. THOMAS, *J. Polym. Sci.* **10** (1953) 291.
4. A. G. THOMAS, *J. Appl. Polym. Sci.* **3** (1960) 168.
5. A. AHAGON, A. N. GENT, H. J. KIM and Y. KUMAGAI, *Rubb. Chem. Technol.* **48** (1975) 896.
6. G. E. ANDERTON and L. R. G. TRELOAR, *J. Mater. Sci.* **6** (1971) 562.
7. G. L. A. SIMS, *J. Mater. Sci.* **10** (1975) 647.
8. P. I. VINCENT, in "Encyclopedia of Polymer Science and Technology", Vol. 7, edited by N. M. Bikales (Interscience, New York, 1967) p. 292.
9. A. K. BHOWMICK and A. N. GENT, *Rubb. Chem. Technol.* **56** (1983) 845.
10. A. K. BHOWMICK, *J. Mater. Sci.* **21** (1986) 3927.
11. T. L. SMITH, *J. Polym. Sci.* **A1** (1963) 3597.
12. *Idem, ibid.* **32** (1958) 99.
13. E. H. ANDREWS (ed.), "Developments in Polymer Fracture I" (Applied Science, London, 1979).
14. N. ROY CHOUDHURY and A. K. BHOWMICK, *J. Appl. Polym. Sci.* **37** (1989) in press.
15. D. S. CHIU, A. N. GENT and J. R. WHITE, *J. Mater. Sci.* **19** (1984) 2622.
16. A. SAHA DEURI and A. K. BHOWMICK, *ibid.* **22** (1987) 4299.
17. T. L. SMITH, *Rubb. Chem. Technol.* **51** (1978) 225.

Received 13 May
and accepted 4 November 1988